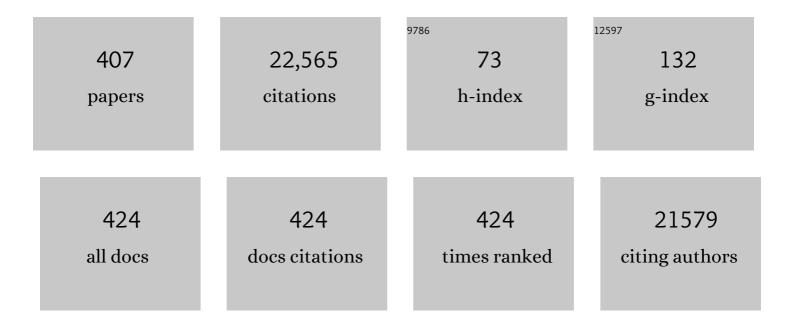
Jan Skov Pedersen

List of Publications by Year in descending order

Source: https://exaly.com/author-pdf/6112852/publications.pdf Version: 2024-02-01



#	Article	IF	CITATIONS
1	Self-assembly of a nanoscale DNA box with a controllable lid. Nature, 2009, 459, 73-76.	27.8	1,464
2	Analysis of small-angle scattering data from colloids and polymer solutions: modeling and least-squares fitting. Advances in Colloid and Interface Science, 1997, 70, 171-210.	14.7	1,423
3	Structural study on the micelle formation of poly(ethylene oxide)-poly(propylene) Tj ETQq1 1 0.784314 rgBT /Ov	verlock 10 4.8	Tf 50 662 Td
4	Scattering Functions of Semiflexible Polymers with and without Excluded Volume Effects. Macromolecules, 1996, 29, 7602-7612.	4.8	535
5	Small-angle neutron scattering study of structural changes in temperature sensitive microgel colloids. Journal of Chemical Physics, 2004, 120, 6197-6206.	3.0	501
6	Scattering Form Factor of Block Copolymer Micelles. Macromolecules, 1996, 29, 1363-1365.	4.8	422
7	Analytical treatment of the resolution function for small-angle scattering. Journal of Applied Crystallography, 1990, 23, 321-333.	4.5	419
8	Self-Healing Mussel-Inspired Multi-pH-Responsive Hydrogels. Biomacromolecules, 2013, 14, 297-301.	5.4	399
9	Determination of size distribution from small-angle scattering data for systems with effective hard-sphere interactions. Journal of Applied Crystallography, 1994, 27, 595-608.	4.5	388
10	Structure of the Exon Junction Core Complex with a Trapped DEAD-Box ATPase Bound to RNA. Science, 2006, 313, 1968-1972.	12.6	365
11	Form factors of block copolymer micelles with spherical, ellipsoidal and cylindrical cores. Journal of Applied Crystallography, 2000, 33, 637-640.	4.5	293
12	Are Thermoresponsive Microgels Model Systems for Concentrated Colloidal Suspensions? A Rheology and Small-Angle Neutron Scattering Study. Langmuir, 2004, 20, 7283-7292.	3.5	247
13	Coherent Nanotwins and Dynamic Disorder in Cesium Lead Halide Perovskite Nanocrystals. ACS Nano, 2017, 11, 3819-3831.	14.6	246
14	The Role of Stable α-Synuclein Oligomers in the Molecular Events Underlying Amyloid Formation. Journal of the American Chemical Society, 2014, 136, 3859-3868.	13.7	218
15	A flux- and background-optimized version of the NanoSTAR small-angle X-ray scattering camera for solution scattering. Journal of Applied Crystallography, 2004, 37, 369-380.	4.5	215
16	Sphere, Cylinder, and Vesicle Nanoaggregates in Poly(styrene-b-isoprene) Diblock Copolymer Solutions. Macromolecules, 2006, 39, 1199-1208.	4.8	211
17	Association behavior of native ?-lactoglobulin. , 1999, 49, 11-20.		186
18	SDS-Induced Fibrillation of α-Synuclein: An Alternative Fibrillation Pathway. Journal of Molecular Biology, 2010, 401, 115-133.	4.2	182

DE

#	Article	IF	CITATIONS
19	Structure of the haptoglobin–haemoglobin complex. Nature, 2012, 489, 456-459.	27.8	180
20	Conformation of Cylindrical Brushes in Solution:Â Effect of Side Chain Length. Macromolecules, 2006, 39, 8440-8450.	4.8	179
21	Structure of Multiresponsive "Intelligent―Coreâ^'Shell Microgels. Journal of the American Chemical Society, 2005, 127, 9372-9373.	13.7	174
22	How Epigallocatechin Gallate Can Inhibit α-Synuclein Oligomer Toxicity in Vitro. Journal of Biological Chemistry, 2014, 289, 21299-21310.	3.4	172
23	Structure of pure SDS and DTAB micelles in brine determined by small-angle neutron scattering (SANS). Physical Chemistry Chemical Physics, 1999, 1, 4437-4446.	2.8	168
24	A Small-Angle Neutron and X-ray Contrast Variation Scattering Study of the Structure of Block Copolymer Micelles:  Corona Shape and Excluded Volume Interactions. Macromolecules, 2003, 36, 416-433.	4.8	168
25	Soft Interactions at Nanoparticles Alter Protein Function and Conformation in a Size Dependent Manner. Nano Letters, 2011, 11, 4985-4991.	9.1	157
26	Temperature-Sensitive Core–Shell Microgel Particles with Dense Shell. Angewandte Chemie - International Edition, 2006, 45, 1737-1741.	13.8	155
27	Mechanism of Trypanosoma brucei gambiense resistance to human serum. Nature, 2013, 501, 430-434.	27.8	150
28	Scattering from block copolymer micelles. Current Opinion in Colloid and Interface Science, 2002, 7, 158-166.	7.4	147
29	Structure of eEF3 and the mechanism of transfer RNA release from the E-site. Nature, 2006, 443, 663-668.	27.8	147
30	A SAXS Study of Glucagon Fibrillation. Journal of Molecular Biology, 2009, 387, 147-161.	4.2	145
31	Aggregation and network formation of aqueous methylcellulose and hydroxypropylmethylcellulose solutions. Colloids and Surfaces A: Physicochemical and Engineering Aspects, 2010, 354, 162-171.	4.7	138
32	Structure factors effects in small-angle scattering from block copolymer micelles and star polymers. Journal of Chemical Physics, 2001, 114, 2839-2846.	3.0	135
33	The Role of Decorated SDS Micelles in Sub-CMC Protein Denaturation and Association. Journal of Molecular Biology, 2009, 391, 207-226.	4.2	130
34	The structure of P85 Pluronic block copolymer micelles determined by small-angle neutron scattering. Colloids and Surfaces A: Physicochemical and Engineering Aspects, 2003, 213, 175-187.	4.7	129
35	SAXS investigation of a cubic to a sponge (L ₃) phase transition in self-assembled lipid nanocarriers. Physical Chemistry Chemical Physics, 2011, 13, 3073-3081.	2.8	128
36	Small-Angle Neutron Scattering (SANS) Study of Vesicles and Lamellar Sheets Formed from Mixtures of an Anionic and a Cationic Surfactant. Journal of Physical Chemistry B, 1999, 103, 9888-9897.	2.6	123

#	Article	IF	CITATIONS
37	Influence of Shell Thickness and Cross-Link Density on the Structure of Temperature-Sensitive Poly-N-Isopropylacrylamideâ^'Poly-N-Isopropylmethacrylamide Coreâ^'Shell Microgels Investigated by Small-Angle Neutron Scattering. Langmuir, 2006, 22, 459-468.	3.5	122
38	Structure of Micelles of a Nonionic Block Copolymer Determined by SANS and SAXS. Journal of Physical Chemistry B, 2011, 115, 11318-11329.	2.6	122
39	Formation of Polymerlike Mixed Micelles and Vesicles in Lecithin-Bile Salt Solutions: A Small-Angle Neutron-Scattering Study. The Journal of Physical Chemistry, 1995, 99, 1299-1305.	2.9	121
40	Structure of and influence of a tick complement inhibitor on human complement component 5. Nature Immunology, 2008, 9, 753-760.	14.5	121
41	Analysis of neutron and X-ray reflectivity data. II. Constrained least-squares methods. Journal of Applied Crystallography, 1994, 27, 36-49.	4.5	117
42	Use of Synthetic Polymers and Biopolymers for Soil Stabilization in Agricultural, Construction, and Military Applications. Journal of Materials in Civil Engineering, 2007, 19, 58-66.	2.9	113
43	Assembly and structural analysis of a covalently closed nano-scale DNA cage. Nucleic Acids Research, 2008, 36, 1113-1119.	14.5	112
44	Structural Development of Self Nano Emulsifying Drug Delivery Systems (SNEDDS) During In Vitro Lipid Digestion Monitored by Small-angle X-ray Scattering. Pharmaceutical Research, 2007, 24, 1844-1853.	3.5	109
45	Small-angle neutron scattering and differential scanning calorimetry studies on the copper clustering stage of Fe–Si–B–Nb–Cu nanocrystalline alloys. Acta Materialia, 2000, 48, 4783-4790.	7.9	105
46	Instrumental Smearing Effects in Radially Symmetric Small-Angle Neutron Scattering by Numerical and Analytical Methods. Journal of Applied Crystallography, 1995, 28, 105-114.	4.5	103
47	Characterization of nanosized partly crystalline photocatalysts. Journal of Nanoparticle Research, 2004, 6, 519-526.	1.9	103
48	Small-Angle Neutron Scattering Study of the Growth Behavior, Flexibility, and Intermicellar Interactions of Wormlike SDS Micelles in NaBr Aqueous Solutions. Langmuir, 2002, 18, 5343-5353.	3.5	102
49	Determination of size distributions in nanosized powders by TEM, XRD, and SAXS. Journal of Experimental Nanoscience, 2006, 1, 355-373.	2.4	102
50	Temperature Sensitive Copolymer Microgels with Nanophase Separated Structure. Journal of the American Chemical Society, 2009, 131, 3093-3097.	13.7	100
51	Static structure factor of polymerlike micelles: Overall dimension, flexibility, and local properties of lecithin reverse micelles in deuterated isooctane. Physical Review E, 1997, 56, 5772-5788.	2.1	98
52	Formation of Tablet-Shaped and Ribbonlike Micelles in Mixtures of an Anionic and a Cationic Surfactant. Langmuir, 1999, 15, 2250-2253.	3.5	98
53	Monitoring the Transition from Spherical to Polymerâ€like Surfactant Micelles Using Smallâ€Angle Xâ€Ray Scattering. Angewandte Chemie - International Edition, 2014, 53, 11524-11528.	13.8	98
54	Silver Nanoparticle Formation in Microemulsions Acting Both as Template and Reducing Agent. Langmuir, 2005, 21, 11387-11396.	3.5	96

#	Article	IF	CITATIONS
55	Frustrated pyrochlore oxides,Y2Mn2O7,Ho2Mn2O7, andYb2Mn2O7: Bulk magnetism and magnetic microstructure. Physical Review B, 1996, 54, 7189-7200.	3.2	93
56	Flexibility of Charged and Uncharged Polymer-like Micelles. Langmuir, 1998, 14, 6013-6024.	3.5	92
57	Micelles and gels of oxyethylene–oxybutylene diblock copolymers in aqueous solution: The effect of oxyethylene-block length. Physical Chemistry Chemical Physics, 1999, 1, 2773-2785.	2.8	91
58	Small-angle scattering from precipitates: Analysis by use of a polydisperse hard-sphere model. Physical Review B, 1993, 47, 657-665.	3.2	90
59	Time-resolved structural evolution during the collapse of responsive hydrogels: The microgel-to-particle transition. Science Advances, 2018, 4, eaao7086.	10.3	90
60	Multi-Shell Hollow Nanogels with Responsive Shell Permeability. Scientific Reports, 2016, 6, 22736.	3.3	89
61	Microstructures and magnetic properties of Co–Al–O granular thin films. Journal of Applied Physics, 2000, 87, 817-823.	2.5	86
62	Ge(111) : The atomic geometry. Surface Science, 1986, 178, 927-933.	1.9	85
63	Surface structure and long-range order of the Ge(111)-c(2×8) reconstruction. Physical Review B, 1988, 38, 9715-9720.	3.2	85
64	Improvements and considerations for size distribution retrieval from small-angle scattering data by Monte Carlo methods. Journal of Applied Crystallography, 2013, 46, 365-371.	4.5	83
65	Mesoporous silica nanoparticles carrying multiple antibiotics provide enhanced synergistic effect and improved biocompatibility. Colloids and Surfaces B: Biointerfaces, 2019, 175, 498-508.	5.0	83
66	Critical Size of Crystalline ZrO ₂ Nanoparticles Synthesized in Near- and Supercritical Water and Supercritical Isopropyl Alcohol. ACS Nano, 2008, 2, 1058-1068.	14.6	82
67	Analysis of neutron and X-ray reflectivity data. I. Theory. Journal of Applied Crystallography, 1994, 27, 29-35.	4.5	80
68	Structure and activation of C1, the complex initiating the classical pathway of the complement cascade. Proceedings of the National Academy of Sciences of the United States of America, 2017, 114, 986-991.	7.1	80
69	Anisotropic Crystal Growth Kinetics of Anatase TiO ₂ Nanoparticles Synthesized in a Nonaqueous Medium. Chemistry of Materials, 2010, 22, 6044-6055.	6.7	77
70	Small-angle X-ray and neutron scattering. Nature Reviews Methods Primers, 2021, 1, .	21.2	77
71	Structure of casein micelles studied by small-angle neutron scattering. European Biophysics Journal, 1996, 24, 143.	2.2	76
72	Contrast Variation Small-Angle Neutron Scattering Study of the Structure of Block Copolymer Micelles in a Slightly Selective Solvent at Semidilute Concentrations. Macromolecules, 2000, 33, 542-550.	4.8	76

#	Article	IF	CITATIONS
73	Adsorbate registry and subsurface relaxation of the reconstructions. Surface Science, 1987, 189-190, 1047-1054.	1.9	75
74	Apparent Specific Volume Measurements of Poly(ethylene oxide), Poly(butylene oxide), Poly(propylene) Tj ETQo Chemistry B, 2004, 108, 6242-6249.	0 0 0 rgB1 2.6	Г /Overlock 10 74
75	Direct Observation of the Formation of Surfactant Micelles under Nonisothermal Conditions by Synchrotron SAXS. Journal of the American Chemical Society, 2013, 135, 7214-7222.	13.7	74
76	Supercritical Propanol–Water Synthesis and Comprehensive Size Characterisation of Highly Crystalline anatase TiO2 Nanoparticles. Journal of Solid State Chemistry, 2006, 179, 2674-2680.	2.9	73
77	Small-Angle X-ray and Neutron Scattering from Bulk and Oriented Triblock Copolymer Gels. Macromolecules, 1995, 28, 2054-2062.	4.8	72
78	Small-Angle Neutron Scattering (SANS) Study of Aggregates Formed from Aqueous Mixtures of Sodium Dodecyl Sulfate (SDS) and Dodecyltrimethylammonium Bromide (DTAB). Langmuir, 1998, 14, 3754-3761.	3.5	72
79	A comparison of three different methods for analysing small-angle scattering data. Journal of Applied Crystallography, 1991, 24, 541-548.	4.5	70
80	Characterization of exfoliated layered double hydroxide (LDH, Mg/Al = 3) nanosheets at high concentrations in formamide. Journal of Materials Chemistry, 2007, 17, 965-971.	6.7	69
81	In Situ High-Energy Synchrotron Radiation Study of Sol–Gel Nanoparticle Formation in Supercritical Fluids. Angewandte Chemie - International Edition, 2007, 46, 1113-1116.	13.8	69
82	Effect of particle size and Debye length on order parameters of colloidal silica suspensions under confinement. Soft Matter, 2011, 7, 10899.	2.7	69
83	Cross-Section Structure of Cylindrical and Polymer-Like Micelles from Small-Angle Scattering Data. I. Test of Analysis Methods. Journal of Applied Crystallography, 1996, 29, 646-661.	4.5	68
84	Potent α-Synuclein Aggregation Inhibitors, Identified by High-Throughput Screening, Mainly Target the Monomeric State. Cell Chemical Biology, 2018, 25, 1389-1402.e9.	5.2	68
85	Neutron diffraction from the vortex lattice in the heavy-fermion superconductorUPt3. Physical Review Letters, 1992, 69, 3120-3123.	7.8	67
86	A Small-Angle Neutron Scattering (SANS) Study of Tablet-Shaped and Ribbonlike Micelles Formed from Mixtures of an Anionic and a Cationic Surfactant. Journal of Physical Chemistry B, 1999, 103, 8502-8513.	2.6	67
87	Synergistic activation of eIF4A by eIF4B and eIF4G. Nucleic Acids Research, 2011, 39, 2678-2689.	14.5	67
88	High Stability and Cooperative Unfolding of α-Synuclein Oligomers. Biochemistry, 2014, 53, 6252-6263.	2.5	67
89	Monte Carlo study of excluded volume effects in wormlike micelles and semiflexible polymers. Physical Review E, 1996, 54, R5917-R5920.	2.1	66
90	Static properties of polystyrene in semidilute solutions: A comparison of Monte Carlo simulation and small-angle neutron scattering results. Europhysics Letters, 1999, 45, 666-672.	2.0	65

#	Article	IF	CITATIONS
91	Droplet polydispersity and shape fluctuations in AOT [bis(2-ethylhexyl)sulfosuccinate sodium salt] microemulsions studied by contrast variation small-angle neutron scattering. Physical Review E, 2001, 63, 061406.	2.1	65
92	Form Factors of Block Copolymer Micelles with Excluded-Volume Interactions of the Corona Chains Determined by Monte Carlo Simulations. Macromolecules, 2002, 35, 1028-1037.	4.8	65
93	Micellar Ordering in Concentrated Solutions of Di- and Triblock Copolymers in a Slightly Selective Solvent. Macromolecules, 1998, 31, 1188-1196.	4.8	64
94	Kinetics of the Formation of 2D-Hexagonal Silica Nanostructured Materials by Nonionic Block Copolymer Templating in Solution. Journal of Physical Chemistry B, 2011, 115, 11330-11344.	2.6	64
95	Model-independent determination of the surface scattering-length-density profile from specular reflectivity data. Journal of Applied Crystallography, 1992, 25, 129-145.	4.5	62
96	Structure and Dynamics of Concentrated Solutions of Asymmetric Block Copolymers in Slightly Selective Solvents. Macromolecules, 1996, 29, 5955-5964.	4.8	62
97	A new small-angle X-ray scattering set-up on theÂcrystallography beamline 1711 at MAX-lab. Journal of Synchrotron Radiation, 2009, 16, 498-504.	2.4	62
98	Rupturing Polymeric Micelles with Cyclodextrins. Langmuir, 2007, 23, 460-466.	3.5	61
99	Structural Insight into the Function of Myelin Basic Protein as a Ligand for Integrin αMβ2. Journal of Immunology, 2008, 180, 3946-3956.	0.8	61
100	Characterization of Prototype Self-Nanoemulsifying Formulations of Lipophilic Compounds. Journal of Pharmaceutical Sciences, 2007, 96, 876-892.	3.3	60
101	A Small-Angle Neutron Scattering Study of Spherical and Wormlike Micelles Formed by Poly(oxyethylene)-Based Diblock Copolymers. Langmuir, 2001, 17, 6386-6388.	3.5	58
102	Cross-Section Structure of Cylindrical and Polymer-like Micelles from Small-Angle Scattering Data. 2. Experimental Results. Langmuir, 1996, 12, 2433-2440.	3.5	56
103	Rheological and Structural Characterization of Hydrophobically Modified Polyacrylamide Solutions in the Semidilute Regime. Macromolecules, 2004, 37, 1492-1501.	4.8	56
104	Effect of Polymer Charge and Geometrical Confinement on Ion Distribution and the Structuring in Semidilute Polyelectrolyte Solutions:  Comparison between AFM and SAXS. Macromolecules, 2006, 39, 7364-7371.	4.8	56
105	Modeling in Situ Small-Angle X-ray Scattering Measurements Following the Formation of Mesostructured Silica. Journal of Physical Chemistry C, 2009, 113, 7706-7713.	3.1	56
106	How Hollow Are Thermoresponsive Hollow Nanogels?. Macromolecules, 2014, 47, 8700-8708.	4.8	56
107	In-Situ Synchrotron Radiation Study of Formation and Growth of Crystalline CexZr1â^'xO2 Nanoparticles Synthesized in Supercritical Water. Chemistry of Materials, 2010, 22, 1814-1820.	6.7	55
108	Structural features and adsorption behaviour of mesoporous silica particles formed from droplets generated in a spraying chamber. Microporous and Mesoporous Materials, 2004, 72, 175-183.	4.4	54

#	Article	IF	CITATIONS
109	Mixtures of n-dodecyl-β-d-maltoside and hexaoxyethylene dodecyl ether — Surface properties, bulk properties, foam films, and foams. Advances in Colloid and Interface Science, 2010, 155, 5-18.	14.7	54
110	Structure and Interactions of Block Copolymer Micelles of Brij 700 Studied by Combining Small-Angle X-ray and Neutron Scattering. Langmuir, 2005, 21, 2137-2149.	3.5	53
111	Conformational Changes in Mannan-Binding Lectin Bound to Ligand Surfaces. Journal of Immunology, 2007, 178, 3016-3022.	0.8	53
112	New routes to food gels and glasses. Faraday Discussions, 2012, 158, 267.	3.2	52
113	Pb/Ge(111)1×1: An anisotropic two-dimensional liquid. Physical Review B, 1990, 41, 9519-9522.	3.2	51
114	Analysis of neutron and X-ray reflectivity data by constrained least-squares methods. Physica B: Condensed Matter, 1994, 198, 16-23.	2.7	51
115	Wormlike Micelles as "Equilibrium Polyelectrolytesâ€⊧ Light and Neutron Scattering Experiments. Langmuir, 2002, 18, 2495-2505.	3.5	51
116	A complete picture of protein unfolding and refolding in surfactants. Chemical Science, 2020, 11, 699-712.	7.4	51
117	Temperature-Induced Ultradense PEG Polyelectrolyte Surface Grafting Provides Effective Long-Term Bioresistance against Mammalian Cells, Serum, and Whole Blood. Biomacromolecules, 2012, 13, 3668-3677.	5.4	50
118	Scattering from Polymerlike Micelles of TDAO in Salt/Water Solutions at Semidilute Concentrations. Langmuir, 2000, 16, 6431-6437.	3.5	48
119	Structural Insights into the Initiating Complex of the Lectin Pathway of Complement Activation. Structure, 2015, 23, 342-351.	3.3	48
120	Magnetic phase diagram of MnSi. Journal of Magnetism and Magnetic Materials, 1995, 140-144, 119-120.	2.3	47
121	Structure of Nanoscale Truncated Octahedral DNA Cages: Variation of Single-Stranded Linker Regions and Influence on Assembly Yields. ACS Nano, 2010, 4, 1367-1376.	14.6	47
122	Tailoring Membrane Nanostructure and Charge Density for High Electrokinetic Energy Conversion Efficiency. ACS Nano, 2016, 10, 2415-2423.	14.6	47
123	Analysis of small-angle scattering data from micelles and microemulsions: free-form approaches and model fitting. Current Opinion in Colloid and Interface Science, 1999, 4, 190-196.	7.4	46
124	A Small-Angle X-ray Scattering Study of Complexes Formed in Mixtures of a Cationic Polyelectrolyte and an Anionic Surfactant. Journal of Physical Chemistry B, 2002, 106, 11412-11419.	2.6	46
125	Lipidoid-polymer hybrid nanoparticles loaded with TNF siRNA suppress inflammation after intra-articular administration in a murine experimental arthritis model. European Journal of Pharmaceutics and Biopharmaceutics, 2019, 142, 38-48.	4.3	46
126	Scattering functions of semidilute solutions of polymers in a good solvent. Journal of Polymer Science, Part B: Polymer Physics, 2004, 42, 3081-3094.	2.1	45

#	Article	IF	CITATIONS
127	H3 and H4 Histone Tails Play a Central Role in the Interactions of Recombinant NCPs. Biophysical Journal, 2007, 92, 2633-2645.	0.5	45
128	Cooperative binding of LysM domains determines the carbohydrate affinity of a bacterial endopeptidase protein. FEBS Journal, 2014, 281, 1196-1208.	4.7	45
129	High Electrokinetic Energy Conversion Efficiency in Charged Nanoporous Nitrocellulose/Sulfonated Polystyrene Membranes. Nano Letters, 2015, 15, 1158-1165.	9.1	45
130	Wormlike Micelle Formation and Flow Alignment of a Pluronic Block Copolymer in Aqueous Solution. Langmuir, 2007, 23, 6896-6902.	3.5	44
131	Reducing Nitrogen Dosage in Triticum durum Plants with Urea-Doped Nanofertilizers. Nanomaterials, 2020, 10, 1043.	4.1	44
132	Cu clustering stage before the crystallization in Feî—,Siî—,Bî—,Nbî—,Cu amorphous alloys. Scripta Materialia, 1999, 12, 693-696.	0.5	43
133	Growth Behavior of Mixed Wormlike Micelles:Â a Small-Angle Scattering Study of the Lecithinâ `Bile Salt System. Langmuir, 2003, 19, 4096-4104.	3.5	43
134	Strontium and Bone Nanostructure in Normal and Ovariectomized Rats Investigated by Scanning Small-Angle X-Ray Scattering. Calcified Tissue International, 2010, 86, 294-306.	3.1	43
135	Crystal structure of a transfer-ribonucleoprotein particle that promotes asparagine formation. EMBO Journal, 2010, 29, 3118-3129.	7.8	43
136	Formation of Dynamic Soluble Surfactant-induced Amyloid β Peptide Aggregation Intermediates. Journal of Biological Chemistry, 2013, 288, 23518-23528.	3.4	43
137	Refolding of SDS-Unfolded Proteins by Nonionic Surfactants. Biophysical Journal, 2017, 112, 1609-1620.	0.5	43
138	Resolution function and flux at the sample for small-angle X-ray scattering calculated in position–angle–wavelength space. Journal of Applied Crystallography, 1991, 24, 893-909.	4.5	42
139	A SANS investigation on absolute scale of a homologous series of base-catalysed silica aerogels. Journal of Non-Crystalline Solids, 1992, 145, 128-132.	3.1	42
140	Analysis of the conformation of worm-like chains by small-angle scattering: Monte-Carlo simulations in comparison to analytical theory. Macromolecular Theory and Simulations, 2000, 9, 345-353.	1.4	41
141	A Small-Angle Neutron Scattering Study of Surfactant Aggregates Formed in Aqueous Mixtures of Sodium Dodecyl Sulfate and Didodecyldimethylammonium Bromide. Journal of Physical Chemistry B, 2000, 104, 4155-4163.	2.6	41
142	Monte Carlo Simulation Study of Concentration Effects and Scattering Functions for Polyelectrolyte Wormlike Micelles. Langmuir, 2002, 18, 2922-2932.	3.5	41
143	The synergic role of collagen and citrate in stabilizing amorphous calcium phosphate precursors with platy morphology. Acta Biomaterialia, 2017, 49, 555-562.	8.3	41
144	Structure of randomly crosslinked poly(dimethylsiloxane) networks produced by electron irradiation. Macromolecules, 1993, 26, 5350-5364.	4.8	40

#	Article	IF	CITATIONS
145	Selfâ€Assembly of a Modified Amyloid Peptide Fragment: pHâ€Responsiveness and Nematic Phase Formation. Macromolecular Bioscience, 2010, 10, 40-48.	4.1	40
146	The Laminin 511/521–binding site on the Lutheran blood group glycoprotein is located at the flexible junction of Ig domains 2 and 3. Blood, 2007, 110, 3398-3406.	1.4	39
147	Simple model for the growth behaviour of mixed lecithin–bile salt micelles. Physical Chemistry Chemical Physics, 2011, 13, 3171-3178.	2.8	39
148	The Role of Nanometer-Scaled Ligand Patterns in Polyvalent Binding by Large Mannan-Binding Lectin Oligomers. Journal of Immunology, 2012, 188, 1292-1306.	0.8	39
149	A small-angle neutron scattering investigation of the structure of highly swollen block copolymer micelles. Journal of Chemical Physics, 2002, 117, 8124-8129.	3.0	38
150	Propagating errors in small-angle scattering data treatment. Journal of Applied Crystallography, 1994, 27, 241-248.	4.5	37
151	Gaussian deconvolution: a useful method for a form-free modeling of scattering data from mono- and multilayered planar systems. Journal of Applied Crystallography, 2012, 45, 1278-1286.	4.5	37
152	Surface charge of acidic sophorolipid micelles: effect of base and time. Soft Matter, 2013, 9, 4911.	2.7	37
153	Generic Structures of Cytotoxic Liprotides: Nanoâ€6ized Complexes with Oleic Acid Cores and Shells of Disordered Proteins. ChemBioChem, 2014, 15, 2693-2702.	2.6	37
154	Small-angle neutron scattering study of a magnetically inhomogeneous amorphous alloy with reentrant behavior. Physical Review B, 2005, 71, .	3.2	36
155	Anisotropic Hollow Microgels That Can Adapt Their Size, Shape, and Softness. Nano Letters, 2019, 19, 8161-8170.	9.1	36
156	Effects of Protonation on Tetradecyldimethylamine Oxide Micelles. Journal of Physical Chemistry B, 2000, 104, 6174-6180.	2.6	35
157	On the Formation Mechanism of Pluronic-Templated Mesostructured Silica. Journal of Physical Chemistry C, 2010, 114, 3483-3492.	3.1	35
158	GGA Autoinhibition Revisited. Traffic, 2010, 11, 259-273.	2.7	34
159	Structure, Aggregation, and Activity of a Covalent Insulin Dimer Formed During Storage of Neutral Formulation of Human Insulin. Journal of Pharmaceutical Sciences, 2016, 105, 1376-1386.	3.3	34
160	Bone Nanostructure near Titanium and porous Tantalum implants studied by Scanning small angle x-ray scattering. , 2006, 12, 81-91.		34
161	Size-Dependent Fault-Driven Relaxation and Faceting in Zincblende CdSe Colloidal Quantum Dots. ACS Nano, 2018, 12, 12558-12570.	14.6	33
162	Orientational ordering in the nematic phase of a thermotropic liquid crystal: A small angle neutron scattering study. Journal of Chemical Physics, 1996, 104, 10046-10054.	3.0	32

#	Article	IF	CITATIONS
163	A novel explanation for the enhanced colloidal stability of silver nanoparticles in the presence of an oppositely charged surfactant. Physical Chemistry Chemical Physics, 2017, 19, 28037-28043.	2.8	32
164	Surface relaxation by the keating model: A comparison with ab-initio calculations aind x-ray diffraction experiments. Surface Science, 1989, 210, 238-250.	1.9	31
165	Surface induced ordering of micelles at the solid-liquid interface. Physical Review E, 1998, 58, 8028-8031.	2.1	31
166	Structural Properties of β-Dodecylmaltoside and C ₁₂ E ₆ Mixed Micelles. Langmuir, 2009, 25, 7296-7303.	3.5	30
167	Plant Polyphenols Inhibit Functional Amyloid and Biofilm Formation in Pseudomonas Strains by Directing Monomers to Off-Pathway Oligomers. Biomolecules, 2019, 9, 659.	4.0	30
168	The C-terminal tail of α-synuclein protects against aggregate replication but is critical for oligomerization. Communications Biology, 2022, 5, 123.	4.4	30
169	Solution scattering structural analysis of the 70 S Escherichia coli ribosome by contrast variation. I. invariants and validation of electron microscopy models 1 1Edited by M. F. Moody. Journal of Molecular Biology, 1997, 271, 588-601.	4.2	29
170	Measuring the exchange-stiffness constant of nanocrystalline solids by elastic small-angle neutron scattering. Philosophical Magazine Letters, 2000, 80, 785-792.	1.2	29
171	Bottle-brush polymers: Adsorption at surfaces and interactions with surfactants. Advances in Colloid and Interface Science, 2010, 155, 50-57.	14.7	29
172	A comprehensive study of the crystallization mechanism involved in the nonaqueous formation of tungstite. Nanoscale, 2013, 5, 8517.	5.6	29
173	Strong interactions with polyethylenimine-coated human serum albumin nanoparticles (PEI-HSA NPs) alter α-synuclein conformation and aggregation kinetics. Nanoscale, 2015, 7, 19627-19640.	5.6	29
174	Myoglobin and α-Lactalbumin Form Smaller Complexes with the Biosurfactant Rhamnolipid Than with SDS. Biophysical Journal, 2017, 113, 2621-2633.	0.5	29
175	Bimodal size distributions of γ′ precipitates in Ni-Al-Mo—I. Small-angle neutron scattering. Acta Metallurgica Et Materialia, 1995, 43, 3427-3439.	1.8	28
176	Block copolymer micelle coronas as quasi-two-dimensional dilute or semidilute polymer solutions. Physical Review E, 2001, 64, 010802.	2.1	28
177	Synthesis and characterization of nanogels of poly(N-isopropylacrylamide) by a combination of light and small-angle X-ray scattering. Physical Chemistry Chemical Physics, 2011, 13, 3108-3114.	2.8	28
178	Silica/alkali ratio dependence of the microscopic structure of sodium silicate solutions. Journal of Colloid and Interface Science, 2013, 397, 9-17.	9.4	28
179	Kinetic Pathways for Polyelectrolyte Coacervate Micelle Formation Revealed by Time-Resolved Synchrotron SAXS. Macromolecules, 2019, 52, 8227-8237.	4.8	28
180	A high-flux automated laboratory small-angle X-ray scattering instrument optimized for solution scattering. Journal of Applied Crystallography, 2021, 54, 295-305.	4.5	28

#	Article	IF	CITATIONS
181	Bimodal size distributions of γ′ precipitates in Ni-Al-Mo—II. Transmission electron microscopy. Acta Metallurgica Et Materialia, 1995, 43, 3441-3451.	1.8	27
182	Small-Angle Scattering Study of TAC8:Â A Surfactant with Cation Complexing Potential. Langmuir, 1997, 13, 1887-1896.	3.5	27
183	Solution scattering structural analysis of the 70 s Escherichia coli ribosome by contrast variation. II †. A model of the ribosome and its RNA at 3.5 nm resolution 1 â€Paper I in this series is the accompanying paper, Svergun et al. (1997) 1Edited by M. F. Moody. Journal of Molecular Biology, 1997, 271, 602-618.	4.2	27
184	Size, flexibility, and scattering functions of semiflexible polyelectrolytes with excluded volume effects: Monte Carlo simulations and neutron scattering experiments. Physical Review E, 2000, 62, 5409-5419.	2.1	27
185	A Monte Carlo study on the effect of excluded volume interactions on the scattering from block copolymer micelles. Journal of Chemical Physics, 2000, 112, 9661-9670.	3.0	27
186	Surface Induced Ordering of Triblock Copolymer Micelles at the Solidâ^'Liquid Interface. 1. Experimental Results. Langmuir, 2002, 18, 4933-4943.	3.5	27
187	Ambiguity in Determining the Shape of Alkali Alkyl Sulfate Micelles from Small-Angle Scattering Data. Langmuir, 2008, 24, 408-417.	3.5	27
188	Protein cage nanoparticles as secondary building units for the synthesis of 3-dimensional coordination polymers. Soft Matter, 2010, 6, 3167.	2.7	27
189	NMR Reveals Two-Step Association of Congo Red to Amyloid β in Low-Molecular-Weight Aggregates. Journal of Physical Chemistry B, 2010, 114, 16003-16010.	2.6	27
190	The effect of PAMAM G6 dendrimers on the structure of lipid vesicles. Physical Chemistry Chemical Physics, 2010, 12, 12267.	2.8	27
191	Effects of Temperature and Salt Concentration on the Structural and Dynamical Features in Aqueous Solutions of Charged Triblock Copolymers. Journal of Physical Chemistry B, 2011, 115, 2125-2139.	2.6	27
192	Structure of Immune Stimulating Complex Matrices and Immune Stimulating Complexes in Suspension Determined by Small-Angle X-Ray Scattering. Biophysical Journal, 2012, 102, 2372-2380.	0.5	27
193	Structural and Functional Characterization of the R-modules in Alginate C-5 Epimerases AlgE4 and AlgE6 from Azotobacter vinelandii. Journal of Biological Chemistry, 2014, 289, 31382-31396.	3.4	27
194	Expansion of the F127-templated mesostructure in aerosol-generated particles by using polypropylene glycol as a swelling agent. Microporous and Mesoporous Materials, 2008, 113, 1-13.	4.4	26
195	Mechanics and dynamics of triglyceride-phospholipid model membranes: Implications for cellular properties and function. Biochimica Et Biophysica Acta - Biomembranes, 2011, 1808, 1947-1956.	2.6	26
196	The structure of the Nâ€ŧerminal module of the cell wall hydrolase RipA and its role in regulating catalytic activity. Proteins: Structure, Function and Bioinformatics, 2018, 86, 912-923.	2.6	26
197	Assessment of structure factors for analysis of small-angle scattering data from desired or undesired aggregates. Journal of Applied Crystallography, 2020, 53, 991-1005.	4.5	26
198	The role of nanoparticle structure and morphology in the dissolution kinetics and nutrient release of nitrate-doped calcium phosphate nanofertilizers. Scientific Reports, 2020, 10, 12396.	3.3	26

#	Article	IF	CITATIONS
199	Bulk amorphous (Mg0.98Al0.02)60Cu30Y10 alloy. Scripta Materialia, 1999, 41, 889-893.	5.2	25
200	Deciphering the Structural Properties That Confer Stability to a DNA Nanocage. ACS Nano, 2009, 3, 1813-1822.	14.6	25
201	In Situ Time-Resolved SAXS Study of the Formation of Mesostructured Organically Modified Silica through Modeling of Micelles Evolution during Surfactant-Templated Self-Assembly. Langmuir, 2012, 28, 17477-17493.	3.5	25
202	Modeling Small-Angle X-ray Scattering Data for Low-Density Lipoproteins: Insights into the Fatty Core Packing and Phase Transition. ACS Nano, 2017, 11, 1080-1090.	14.6	25
203	Anisometric Polyelectrolyte/Mixed Surfactant Nanoassemblies Formed by the Association of Poly(diallyldimethylammonium chloride) with Sodium Dodecyl Sulfate and Dodecyl Maltoside. Langmuir, 2015, 31, 7242-7250.	3.5	24
204	Effect of Temperature and Ionic Strength on Micellar Aggregates of Oppositely Charged Thermoresponsive Block Copolymer Polyelectrolytes. Langmuir, 2019, 35, 13614-13623.	3.5	24
205	Bacterial amphiphiles as amyloid inducers: Effect of Rhamnolipid and Lipopolysaccharide on FapC fibrillation. Biochimica Et Biophysica Acta - Proteins and Proteomics, 2019, 1867, 140263.	2.3	23
206	Predicted Loop Regions Promote Aggregation: A Study of Amyloidogenic Domains in the Functional Amyloid FapC. Journal of Molecular Biology, 2020, 432, 2232-2252.	4.2	23
207	Controlling the morphology of microgels by ionic stimuli. Soft Matter, 2020, 16, 2786-2794.	2.7	23
208	Structural Model of the 50 S Subunit of Escherichia coli Ribosomes from Solution Scattering. Journal of Molecular Biology, 1994, 240, 78-86.	4.2	22
209	Microstructure of Guinier-Preston zones in Alî—,Ag. Acta Materialia, 1996, 44, 4845-4852.	7.9	22
210	Small-angle neutron scattering of precipitates in Ni-rich Niî—,Ti alloys—I. Metastable states in poly- and single crystals. Acta Materialia, 1997, 45, 3311-3318.	7.9	22
211	Composition, structure and properties of POPC–triolein mixtures. Evidence of triglyceride domains in phospholipid bilayers. Biochimica Et Biophysica Acta - Biomembranes, 2013, 1828, 1909-1917.	2.6	22
212	Lowâ€Resolution Structures of OmpAâDDM Protein–Detergent Complexes. ChemBioChem, 2014, 15, 2113-2124.	2.6	22
213	How Peptide Molecular Structure and Charge Influence the Nanostructure of Lipid Bicontinuous Cubic Mesophases: Model Synthetic WALP Peptides Provide Insights. Langmuir, 2016, 32, 6882-6894.	3.5	22
214	Using protein-fatty acid complexes to improve vitamin D stability. Journal of Dairy Science, 2016, 99, 7755-7767.	3.4	22
215	Solution scattering from 50S ribosomal subunit resolves inconsistency between electron microscopic models Proceedings of the National Academy of Sciences of the United States of America, 1994, 91, 11826-11830.	7.1	21
216	Time-Resolved in Situ Small-Angle X-ray Scattering Study of Silica Particle Formation in Nonionic Water-in-Oil Microemulsions. Langmuir, 2008, 24, 5225-5228.	3.5	21

#	Article	IF	CITATIONS
217	Structures of PEP–PEO Block Copolymer Micelles: Effects of Changing Solvent and PEO Length and Comparison to a Thermodynamic Model. Macromolecules, 2012, 45, 430-440.	4.8	21
218	Gallic acid loaded onto polyethylenimine-coated human serum albumin nanoparticles (PEI-HSA-GA NPs) stabilizes α-synuclein in the unfolded conformation and inhibits aggregation. RSC Advances, 2016, 6, 85312-85323.	3.6	21
219	Structural Investigations of Human A2M Identify a Hollow Native Conformation That Underlies Its Distinctive Protease-Trapping Mechanism. Molecular and Cellular Proteomics, 2021, 20, 100090.	3.8	21
220	Scattering from Short Stiff Cylindrical Micelles Formed by Fully Ionized TDAO in NaCl/Water Solutions. Langmuir, 2003, 19, 3656-3665.	3.5	20
221	Small-Angle Neutron Scattering Study of the Structure of Superswollen Micelles Formed by a Highly Asymmetric Poly(oxybutylene)â^Poly(oxyethylene) Diblock Copolymer in Aqueous Solution. Langmuir, 2004, 20, 2992-2994.	3.5	20
222	Mapping of unfolding states of integral helical membrane proteins by GPS-NMR and scattering techniques: TFE-induced unfolding of KcsA in DDM surfactant. Biochimica Et Biophysica Acta - Biomembranes, 2012, 1818, 2290-2301.	2.6	20
223	Coacervates of Lactotransferrin and β- or κ-Casein: Structure Determined Using SAXS. Langmuir, 2013, 29, 10483-10490.	3.5	20
224	Dendrimer Nanofluids in the Concentrated Regime: From Polymer Melts to Soft Spheres. Langmuir, 2015, 31, 3333-3342.	3.5	20
225	Liprotides made of α-lactalbumin and cis fatty acids form core–shell and multi-layer structures with a common membrane-targeting mechanism. Biochimica Et Biophysica Acta - Proteins and Proteomics, 2016, 1864, 847-859.	2.3	20
226	Can a Charged Surfactant Unfold an Uncharged Protein?. Biophysical Journal, 2018, 115, 2081-2086.	0.5	20
227	Effect of pH on the conformation of bovine serume albumin - gold bioconjugates. Journal of Molecular Liquids, 2020, 309, 113065.	4.9	20
228	On the amorphous layer in bone mineral and biomimetic apatite: A combined small- and wide-angle X-ray scattering analysis. Acta Biomaterialia, 2021, 120, 167-180.	8.3	20
229	Temperature Dependence of the Structure and Interaction of Starlike PEG-Based Block Copolymer Micelles. Macromolecules, 2004, 37, 1682-1685.	4.8	19
230	Preparation Temperature Dependence of Size and Polydispersity of Alkylthiol Monolayer Protected Gold Clusters. Langmuir, 2005, 21, 10320-10323.	3.5	19
231	Nanostructure of the neurocentral growth plate: Insight from scanning small angle X-ray scattering, atomic force microscopy and scanning electron microscopy. Bone, 2006, 39, 530-541.	2.9	19
232	A SANS Contrast Variation Study of Microemulsion Droplet Growth. Journal of Physical Chemistry B, 2007, 111, 682-689.	2.6	19
233	SAXS Models of TGFBIp Reveal a Trimeric Structure and Show That the Overall Shape Is Not Affected by the Arg124His Mutation. Journal of Molecular Biology, 2011, 408, 503-513.	4.2	19
234	Variations in Structure Explain the Viscometric Behavior of AOT Microemulsions at Low Water/AOT Molar Ratios. Zeitschrift Fur Physikalische Chemie, 2012, 226, 201-218.	2.8	19

#	Article	IF	CITATIONS
235	Structure and Interactions of Charged Triblock Copolymers Studied by Small-Angle X-ray Scattering: Dependence on Temperature and Charge Screening. Langmuir, 2012, 28, 1105-1114.	3.5	19
236	XTACC3–XMAP215 association reveals an asymmetric interaction promoting microtubule elongation. Nature Communications, 2014, 5, 5072.	12.8	19
237	Protein-Binding RNA Aptamers Affect Molecular Interactions Distantly from Their Binding Sites. PLoS ONE, 2015, 10, e0119207.	2.5	19
238	Small-Angle X-ray Scattering Studies of Thermoresponsive Poly(<i>N</i> -isopropylacrylamide) Star Polymers in Water. Macromolecules, 2015, 48, 2235-2243.	4.8	19
239	Transformation from Globular to Cylindrical Mixed Micelles through Molecular Exchange that Induces Micelle Fusion. Journal of Physical Chemistry Letters, 2016, 7, 2039-2043.	4.6	19
240	Small-angle X-ray scattering studies of metastable intermediates of ?-lactoglobulin isolated after heat-induced aggregation. Biopolymers, 2003, 70, 377-390.	2.4	18
241	Polypeptide Nanoribbon Hydrogels Assembled through Multiple Supramolecular Interactions. Langmuir, 2009, 25, 12899-12908.	3.5	18
242	Structure of PEP–PEO block copolymer micelles: exploiting the complementarity of small-angle X-ray scattering and static light scattering. Journal of Applied Crystallography, 2011, 44, 473-482.	4.5	18
243	Characterisation of fractionated skim milk with small-angle X-ray scattering. International Dairy Journal, 2013, 33, 1-9.	3.0	18
244	Construction of a Polyhedral DNA 12-Arm Junction for Self-Assembly of Wireframe DNA Lattices. ACS Nano, 2017, 11, 9041-9047.	14.6	18
245	Unfolding and partial refolding of a cellulase from the SDS-denatured state: From β-sheet to α-helix and back. Biochimica Et Biophysica Acta - General Subjects, 2020, 1864, 129434.	2.4	18
246	Application of Quality by Design to the robust preparation of a liposomal GLA formulation by DELOS-susp method. Journal of Supercritical Fluids, 2021, 173, 105204.	3.2	18
247	X-ray diffraction study of the Ge(111)5×5-Sn and Ge(111)7×7-Sn surfaces. Physical Review B, 1988, 38, 13210-13221.	3.2	17
248	Ordering of the Disk-like 2,3,6,7,10,11-Hexakis(hexylthio)triphenylene in Solution and at a Liquidâ^'Solid Interface. Langmuir, 1996, 12, 1690-1692.	3.5	17
249	Dependence on Oil Chain Length of the Curvature Elastic Properties of Nonionic Surfactant Films: Emulsification Failure and Phase Equilibria. Journal of Dispersion Science and Technology, 2006, 27, 497-510.	2.4	17
250	Lysophospholipids induce fibrillation of the repeat domain of Pmel17 through intermediate core-shell structures. Biochimica Et Biophysica Acta - Proteins and Proteomics, 2019, 1867, 519-528.	2.3	17
251	On the morphology of a lamellar triblock copolymer film. Journal De Physique II, 1993, 3, 139-146.	0.9	17
252	The Use of Liprotides To Stabilize and Transport Hydrophobic Molecules. Biochemistry, 2015, 54, 4815-4823.	2.5	16

#	Article	IF	CITATIONS
253	Crystal Structure of a Two-domain Fragment of Hepatocyte Growth Factor Activator Inhibitor-1. Journal of Biological Chemistry, 2016, 291, 14340-14355.	3.4	16
254	Impact of Chemical Composition on the Nanostructure and Biological Activity of α-Galactosidase-Loaded Nanovesicles for Fabry Disease Treatment. ACS Applied Materials & Interfaces, 2021, 13, 7825-7838.	8.0	16
255	Electron correlations in organic 1:2-TCNQ salts. Reports on Progress in Physics, 1987, 50, 995-1043.	20.1	15
256	Transparency and wettability of PVP/PDMSâ€IPN synthesized in different organic solvents. Journal of Applied Polymer Science, 2009, 114, 1828-1839.	2.6	15
257	The growth of micelles, and the transition to bilayers, in mixtures of a single-chain and a double-chain cationic surfactant investigated with small-angle neutron scattering. Soft Matter, 2011, 7, 10935.	2.7	15
258	How Glycosaminoglycans Promote Fibrillation of Salmon Calcitonin. Journal of Biological Chemistry, 2016, 291, 16849-16862.	3.4	15
259	The random co-polymer glatiramer acetate rapidly kills primary human leukocytes through sialic-acid-dependent cell membrane damage. Biochimica Et Biophysica Acta - Biomembranes, 2017, 1859, 425-437.	2.6	15
260	α-Synucleins from Animal Species Show Low Fibrillation Propensities and Weak Oligomer Membrane Disruption. Biochemistry, 2018, 57, 5145-5158.	2.5	15
261	Insight into the molecular mechanism behind PEG-mediated stabilization of biofluid lipases. Scientific Reports, 2018, 8, 12293.	3.3	15
262	The changing face of SDS denaturation: Complexes of Thermomyces lanuginosus lipase with SDS at pH 4.0, 6.0 and 8.0. Journal of Colloid and Interface Science, 2022, 614, 214-232.	9.4	15
263	Microemulsion Droplets Decorated by Brij700 Block Copolymer:  Phase Behavior and Structural Investigation by SAXS and SANS. Langmuir, 2007, 23, 6544-6553.	3.5	14
264	Phase Behavior and Microstructure of C ₁₂ E ₅ Nonionic Microemulsions with Chlorinated Oils. Langmuir, 2008, 24, 3111-3117.	3.5	14
265	Simulative Analysis of a Truncated Octahedral DNA Nanocage Family Indicates the Single-Stranded Thymidine Linkers as the Major Player for the Conformational Variability. Journal of Physical Chemistry C, 2011, 115, 16819-16827.	3.1	14
266	Small-Angle X-ray Scattering Study of Charged Triblock Copolymers as a Function of Polymer Concentration, Temperature, and Charge Screening. Macromolecules, 2012, 45, 246-255.	4.8	14
267	Outset of the Morphology of Nanostructured Silica Particles during Nucleation Followed by Ultrasmall-Angle X-ray Scattering. Langmuir, 2016, 32, 5162-5172.	3.5	14
268	Multi-Step Unfolding and Rearrangement of $\hat{I}\pm$ -Lactalbumin by SDS Revealed by Stopped-Flow SAXS. Frontiers in Molecular Biosciences, 2020, 7, 125.	3.5	14
269	Mixed liposomes containing gram-positive bacteria lipids: Lipoteichoic acid (LTA) induced structural changes. Colloids and Surfaces B: Biointerfaces, 2021, 199, 111551.	5.0	14
270	Polydimethylsiloxane Networks at Equilibrium Swelling:Â Extracted and Nonextracted Networks. Macromolecules, 1996, 29, 809-818.	4.8	13

#	Article	IF	CITATIONS
271	Resolution Function for Two-Axis Specular Neutron Reflectivity. Journal of Applied Crystallography, 1996, 29, 152-158.	4.5	13
272	A small angle neutron scattering study of the conformation of a side chain liquid crystal poly(methacrylate) in the smectic C phase. Liquid Crystals, 1997, 22, 679-684.	2.2	13
273	Scattering vector dependence of the small-angle scattering from mixtures of hydrogenated and deuterated organic solvents. Journal of Applied Crystallography, 2000, 33, 650-652.	4.5	13
274	Block-Copolymer Micro-emulsion with Solvent-Induced Segregation. Langmuir, 2007, 23, 2117-2125.	3.5	13
275	Phase Behavior and Kinetics of Phase Separation of a Nonionic Microemulsion of C ₁₂ E ₅ /Water/1-Chlorotetradecane upon a Temperature Quench. Journal of Physical Chemistry B, 2009, 113, 7138-7146.	2.6	13
276	Oxygen Diffusion in Cross-Linked, Ethanol-Swollen Poly(vinyl alcohol) Gels: Counter-Intuitive Results Reflect Microscopic Heterogeneities. Langmuir, 2009, 25, 1148-1153.	3.5	13
277	The Shapes of Z- α 1 -Antitrypsin Polymers in Solution Support the C-Terminal Domain-Swap Mechanism of Polymerization. Biophysical Journal, 2014, 107, 1905-1912.	0.5	13
278	Modelling of high-symmetry nanoscale particles by small-angle scattering. Journal of Applied Crystallography, 2014, 47, 84-94.	4.5	13
279	A self-assembled nanopatch with peptide–organic multilayers and mechanical properties. Nanoscale, 2015, 7, 2250-2254.	5.6	13
280	Mixed micelles of oppositely charged poly(<i>N</i> -isopropylacrylamide) diblock copolymers. Journal of Polymer Science, Part B: Polymer Physics, 2017, 55, 1457-1470.	2.1	13
281	Molecular dynamics study of ACBP denaturation in alkyl sulfates demonstrates possible pathways of unfolding through fused surfactant clusters. Protein Engineering, Design and Selection, 2019, 32, 175-190.	2.1	13
282	The Three-Dimensional Resolution Function for Small-Angle Scattering and Laue Geometries. Journal of Applied Crystallography, 1995, 28, 209-222.	4.5	12
283	Instrumentation for Small-Angle Scattering. , 1995, , 57-91.		12
284	Small-angle neutron scattering behavior of Fe91Zr9 glass under magnetic field. Journal of Applied Physics, 1996, 79, 5146.	2.5	12
285	The Surface-Induced Ordering of Triblock Copolymer Micelles at the Solidâ^'Liquid Interface. 2. Modeling. Langmuir, 2001, 17, 7040-7046.	3.5	12
286	Activation of the Zymogen to Urokinase-Type Plasminogen Activator Is Associated with Increased Interdomain Flexibility. Journal of Molecular Biology, 2011, 411, 417-429.	4.2	12
287	Temperature-Induced Attractive Interactions of PEO-Containing Block Copolymer Micelles. Langmuir, 2014, 30, 6021-6029.	3.5	12
288	Structural Evolution of Aqueous Zirconium Acetate by Time-Resolved Small-Angle X-ray Scattering and Rheology. Journal of Physical Chemistry C, 2015, 119, 12660-12667.	3.1	12

#	Article	IF	CITATIONS
289	Small-Angle X-ray Scattering Demonstrates Similar Nanostructure in Cortical Bone from Young Adult Animals of Different Species. Calcified Tissue International, 2016, 99, 76-87.	3.1	12
290	Glycolipid Biosurfactants Activate, Dimerize, and Stabilize <i>Thermomyces lanuginosus</i> Lipase in a pH-Dependent Fashion. Biochemistry, 2017, 56, 4256-4268.	2.5	12
291	Bacillus Licheniformis CotA Laccase Mutant: ElectrocatalyticReduction of O 2 from 0.6â€V (SHE) at pH 8 and in Seawater. ChemElectroChem, 2019, 6, 2043-2049.	3.4	12
292	Insight into the Structure and Activity of Surfaceâ€Engineered Lipase Biofluids. ChemBioChem, 2019, 20, 1266-1272.	2.6	12
293	Recombinant Human Epidermal Growth Factor/Quatsome Nanoconjugates: A Robust Topical Delivery System for Complex Wound Healing. Advanced Therapeutics, 2021, 4, 2000260.	3.2	12
294	A small-angle neutron scattering and transmission electron microscopy study of krypton precipitates in copper. Journal of Physics Condensed Matter, 1996, 8, 8431-8455.	1.8	11
295	Magnetic small-angle scattering from Cu-17 at.% Mn. Journal of Physics Condensed Matter, 1998, 10, 8395-8400.	1.8	11
296	Divalent Cations and Redox Conditions Regulate the Molecular Structure and Function of Visinin-Like Protein-1. PLoS ONE, 2011, 6, e26793.	2.5	11
297	Waterâ€inâ€Oil Microâ€Emulsion Enhances the Secondary Structure of a Protein by Confinement. ChemPhysChem, 2012, 13, 3179-3184.	2.1	11
298	Formation of Nanostructured Silica Materials Templated with Nonionic Fluorinated Surfactant Followed by in Situ SAXS. Langmuir, 2013, 29, 2007-2023.	3.5	11
299	Liprotides assist in folding of outer membrane proteins. Protein Science, 2018, 27, 451-462.	7.6	11
300	Role of Charge and Hydrophobicity in Liprotide Formation: A Molecular Dynamics Study with Experimental Constraints. ChemBioChem, 2018, 19, 263-271.	2.6	11
301	Structural insights into the substrate-binding proteins Mce1A and Mce4A from <i>Mycobacterium tuberculosis</i> . IUCrJ, 2021, 8, 757-774.	2.2	11
302	Resolution effects and analysis of small-angle neutron scattering data. European Physical Journal Special Topics, 1993, 03, C8-491-C8-498.	0.2	10
303	Structure and flexibility of worm-like micelles. Physica B: Condensed Matter, 1997, 234-236, 273-275.	2.7	10
304	Distribution of Co Particles ini Co-Al-O Granular Thin Films. Materials Science Forum, 1999, 307, 171-176.	0.3	10
305	Temperature-induced aggregation in aqueous solutions of pluronic F68 triblock copolymer containing small amount of o-xylene. Physica B: Condensed Matter, 2000, 276-278, 363-364.	2.7	10
306	A small-angle X-ray scattering study of aggregation and gelation of colloidal silica. Colloids and Surfaces A: Physicochemical and Engineering Aspects, 2008, 315, 23-30.	4.7	10

#	Article	IF	CITATIONS
307	Structural Transitions of Translation Initiation Factor IF2 upon GDPNP and GDP Binding in Solution. Biochemistry, 2011, 50, 9779-9787.	2.5	10
308	A formalism for scattering of complex composite structures. I. Applications to branched structures of asymmetric sub-units. Journal of Chemical Physics, 2012, 136, 104105.	3.0	10
309	Investigation on the structure of temperature-responsive <i>N</i> -isopropylacrylamide microgels containing a new hydrophobic crosslinker. Cogent Chemistry, 2015, 1, 1012658.	2.5	10
310	A multimethod approach for analyzing FapC fibrillation and determining mass per length. Biophysical Journal, 2021, 120, 2262-2275.	0.5	10
311	Self-assembling properties of ionisable amphiphilic drugs in aqueous solution. Journal of Colloid and Interface Science, 2021, 600, 701-710.	9.4	10
312	Folding Steps in the Fibrillation of Functional Amyloid: Denaturant Sensitivity Reveals Common Features in Nucleation and Elongation. Journal of Molecular Biology, 2022, 434, 167337.	4.2	10
313	Shape transformations in biological mixed surfactant systems: from spheres to cylinders to vesicles. , 1995, , 224-227.		9
314	Small-angle neutron-scattering studies of the magnetic phase diagram of MnSi. Physica B: Condensed Matter, 1995, 213-214, 375-377.	2.7	9
315	A small-angle neutron scattering study of the structure of graphitized carbon black aggregates in Triton X-100/water solutions. Colloids and Surfaces A: Physicochemical and Engineering Aspects, 1998, 132, 203-212.	4.7	9
316	Structure of Doubly Temperature Sensitive Core-Shell Microgels Based on Poly-N-Isopropylacrylamide and Poly-N-Isopropylmethacrylamide. , 2006, , 35-40.		9
317	Solution Structure of C-Terminal Escherichia coli Translation Initiation Factor IF2 by Small-Angle X-ray Scattering. Biochemistry, 2008, 47, 5590-5598.	2.5	9
318	Calculation of two-dimensional scattering patterns for oriented systems. Journal of Applied Crystallography, 2017, 50, 840-850.	4.5	9
319	Stabilizing vitamin D3 using the molten globule state of α-lactalbumin. Journal of Dairy Science, 2018, 101, 1817-1826.	3.4	9
320	Real-time monitoring of oil-induced micellar transitions in viscoelastic surfactants by small-angle X-ray scattering. Journal of Colloid and Interface Science, 2020, 580, 399-406.	9.4	9
321	Crystal and solution structures of fragments of the human leucocyte common antigen-related protein. Acta Crystallographica Section D: Structural Biology, 2020, 76, 406-417.	2.3	9
322	Interactions in protein solutions close to liquid–liquid phase separation: ethanol reduces attractions <i>via</i> changes of the dielectric solution properties. Physical Chemistry Chemical Physics, 2021, 23, 22384-22394.	2.8	9
323	Micelles as model systems for equilibrium polyelectrolytes: a light and neutron scattering study. , 2000, , 347-352.		9
324	An Atomistic Model Describing the Structure and Morphology of Cu-Doped C-S-H Hardening Accelerator Nanoparticles. Nanomaterials, 2022, 12, 342.	4.1	9

#	Article	IF	CITATIONS
325	Human myelin proteolipid protein structure and lipid bilayer stacking. Cellular and Molecular Life Sciences, 2022, 79, .	5.4	9
326	Small-angle neutron scattering from poly(NIPA-co-AMPS) gels. Journal of Applied Crystallography, 2000, 33, 735-739.	4.5	8
327	Mechanism of Oligomerisation of Cyclase-associated Protein from Dictyostelium discoideum in Solution. Journal of Molecular Biology, 2006, 362, 1072-1081.	4.2	8
328	The mixture of poly(propylene-glycol)-block-poly(ethylene-glycol)-block-PPG with C12E5microemulsion. Physics and Chemistry of Liquids, 2014, 52, 113-121.	1.2	8
329	Core Freezing and Size Segregation in Surfactant Core–Shell Micelles. Journal of Physical Chemistry B, 2015, 119, 10798-10806.	2.6	8
330	Smallâ€angle Xâ€ray scattering as a useful supplementary technique to determine molecular masses of polyelectrolytes in solution. Journal of Polymer Science, Part B: Polymer Physics, 2016, 54, 1913-1917.	2.1	8
331	Host–guest interaction and structural ordering in polymeric nanoassemblies: Influence of molecular design. International Journal of Pharmaceutics, 2017, 531, 433-443.	5.2	8
332	Structure of Phospholipid Mixed Micelles (Bicelles) Studied by Small-Angle X-ray Scattering. Langmuir, 2018, 34, 14597-14607.	3.5	8
333	Complementary substrate specificity and distinct quaternary assembly of the <i>Escherichia coli</i> aerobic and anaerobic β-oxidation trifunctional enzyme complexes. Biochemical Journal, 2019, 476, 1975-1994.	3.7	8
334	Ubiquitin forms conventional decorated micelle structures with sodium dodecyl sulfate at saturation. Journal of Colloid and Interface Science, 2021, 596, 233-244.	9.4	8
335	Optimum intensity in small-angle neutron scattering. An experimental comparison between symmetric and asymmetric geometries. Journal of Applied Crystallography, 1994, 27, 330-337.	4.5	7
336	Properties of polyelectrolyte chains from analysis of angular correlation functions. Journal of Chemical Physics, 2002, 117, 8973-8982.	3.0	7
337	Investigation of the enhanced ability of bile salt surfactants to solubilize phospholipid bilayers and form mixed micelles. Soft Matter, 2021, 17, 7769-7780.	2.7	7
338	Structure of clathrin-coated vesicles from small-angle scattering experiments. European Biophysics Journal, 1993, 22, 79-95.	2.2	6
339	Guinier-Preston zones in Al-rich Alî—,Cu and Alî—,Ag single crystals. Physica B: Condensed Matter, 1997, 234-236, 983-985.	2.7	6
340	Monte Carlo simulations and analysis of scattering from neutral and polyelectrolyte polymer and polymer-like systems. Current Opinion in Colloid and Interface Science, 2004, 8, 507-514.	7.4	6
341	Decoupling particle formation from intraparticle ordering in mesostructured silica colloids. Microporous and Mesoporous Materials, 2011, 145, 59-64.	4.4	6
342	Phase densities and lamellar morphologies of semicrystalline polyethylenesviaabsolute small-angle X-ray scattering measurements. Journal of Applied Crystallography, 2015, 48, 1498-1506.	4.5	6

#	Article	IF	CITATIONS
343	Formation and properties of nanoemulsions. , 2016, , 193-226.		6
344	Induction, inhibition, and incorporation: Different roles for anionic and zwitterionic lysolipids in the fibrillation of the functional amyloid FapC. Journal of Biological Chemistry, 2022, 298, 101569.	3.4	6
345	Structural Basis for Dityrosine-Mediated Inhibition of α-Synuclein Fibrillization. Journal of the American Chemical Society, 2022, 144, 11949-11954.	13.7	6
346	Membrane composition of polymer-lipid hybrid vesicles. Applied Materials Today, 2022, 29, 101549.	4.3	6
347	Structural Refinement of Ag-Fe Blends during High Energy Ball Milling. Materials Science Forum, 1998, 269-272, 397-402.	0.3	5
348	Microstructural Characterization of Granular CuCo Rapidly Solidified Ribbons. Materials Science Forum, 1998, 269-272, 339-344.	0.3	5
349	Single-coil properties and concentration effects for polyelectrolyte-like wormlike micelles: a Monte Carlo study. Journal of Physics Condensed Matter, 2002, 14, 2283-2295.	1.8	5
350	Nucleation of an Oil Phase in a Nonionic Microemulsion-Containing Chlorinated Oil upon Systematic Temperature Quench. Journal of Physical Chemistry B, 2010, 114, 7769-7776.	2.6	5
351	Structural Analysis of RNA Helicases with Small-Angle X-ray Scattering. Methods in Enzymology, 2012, 511, 191-212.	1.0	5
352	The effect of cationic and anionic blocks on temperature-induced micelle formation. Journal of Applied Crystallography, 2014, 47, 22-28.	4.5	5
353	Release of Solubilizate from Micelle upon Core Freezing. Journal of Physical Chemistry B, 2017, 121, 10353-10363.	2.6	5
354	Effects of Hydration on Structure and Phase Behavior of Pig Gastric Mucin Elucidated by SAXS. Journal of Physical Chemistry B, 2018, 122, 7539-7546.	2.6	5
355	Discovering New Features of Protein Complexes Structures by Small-Angle X-Ray Scattering. Lecture Notes in Physics, 2009, , 231-244.	0.7	5
356	Universal effective interactions of globular proteins close to liquid-liquid phase separation: corresponding-states behavior reflected in the structure factor. Journal of Chemical Physics, 0, , .	3.0	5
357	Neutron scattering experiments on swollen, uniaxially stretched polymer networks. Journal of Molecular Structure, 1996, 383, 69-74.	3.6	4
358	Comment on Correlation effects in small-angle neutron scattering from closely packed spheres by Bertram (1996). Journal of Applied Crystallography, 1998, 31, 488-489.	4.5	4
359	A formalism for scattering of complex composite structures. II. Distributed reference points. Journal of Chemical Physics, 2012, 136, 154907.	3.0	4
360	Structures and mechanisms of formation of liprotides. Biochimica Et Biophysica Acta - Proteins and Proteomics, 2020, 1868, 140505.	2.3	4

#	Article	IF	CITATIONS
361	Toward reliable low-density lipoprotein ultrastructure prediction in clinical conditions: A small-angle X-ray scattering study on individuals with normal and high triglyceride serum levels. Nanomedicine: Nanotechnology, Biology, and Medicine, 2021, 31, 102318.	3.3	4
362	Cys-labeling kinetics of membrane protein GlpG: a role for specific SDS binding and micelle changes?. Biophysical Journal, 2021, 120, 4115-4128.	0.5	4
363	Lattice dynamics of the organic conductors MNEB(TCNQ)2and TEA(TCNQ)2studied by inelastic neutron scattering. Journal of Physics C: Solid State Physics, 1987, 20, 1781-1802.	1.5	3
364	Small-Angle Neutron Scattering from Anisotropic Single-Crystalline Materials. Journal of Applied Crystallography, 1997, 30, 575-579.	4.5	3
365	Moments and distribution function of polyelectrolyte chains. Journal of Chemical Physics, 2004, 120, 8862-8865.	3.0	3
366	Investigating the Effect of Adding Drug (Lidocaine) to aÂDrug Delivery System Using Small-Angle X-Ray Scattering. , 2008, , 101-106.		3
367	Investigation of nanoscale structures by small-angle X-ray scattering in a radiochromic dosimeter. RSC Advances, 2014, 4, 9152.	3.6	3
368	Promoting protein self-association in non-glycosylated Thermomyces lanuginosus lipase based on crystal lattice contacts. Biochimica Et Biophysica Acta - Proteins and Proteomics, 2015, 1854, 1914-1921.	2.3	3
369	Tailoring thermal treatment to form liprotide complexes between oleic acid and different proteins. Biochimica Et Biophysica Acta - Proteins and Proteomics, 2017, 1865, 682-693.	2.3	3
370	Models of the complement C1 complex. Proceedings of the National Academy of Sciences of the United States of America, 2018, 115, E3866-E3866.	7.1	3
371	Mutation-induced dimerization of transforming growth factor-β–induced protein may drive protein aggregation in granular corneal dystrophy. Journal of Biological Chemistry, 2021, 297, 100858.	3.4	3
372	Analysis of the conformation of worm-like chains by small-angle scattering: Monte-Carlo simulations in comparison to analytical theory. Macromolecular Theory and Simulations, 2000, 9, 345-353.	1.4	3
373	Scattering from Wormlike Micelles. Surfactant Science, 2007, , 179-222.	0.0	3
374	Structure and Orientation of the SARS-Coronavirus-2 Spike Protein at Air–Water Interfaces. Journal of Physical Chemistry B, 2022, 126, 3425-3430.	2.6	3
375	Magnetic ordering in pyrochlore Ho2Mn2O7. Journal of Applied Physics, 1996, 79, 6173.	2.5	2
376	Neutron reflectometry from solid-solid and solid-liquid interfaces at the TAS8 spectrometer at risÃ, Neutron News, 1996, 7, 25-30.	0.2	2
377	Structure of Doubly Temperature Sensitive Core-Shell Microgels Based on Poly-N-Isopropylacrylamide and Poly-N-Isopropylmethacrylamide. , 2006, , 35-40.		2
378	Phonons in TCNQ conductors measured by inelastic neutron scattering and their relation to electronic correlation effects. Synthetic Metals, 1987, 19, 433-438.	3.9	1

#	Article	IF	CITATIONS
379	Scaling in the aggregation behaviour of zinc-free insulin studied by small-angle neutron scattering. Nuovo Cimento Della Societa Italiana Di Fisica D - Condensed Matter, Atomic, Molecular and Chemical Physics, Biophysics, 1994, 16, 1447-1455.	0.4	1
380	Architecture of the E.coli 70S ribosome. Physica B: Condensed Matter, 1997, 234-236, 199-201.	2.7	1
381	On the conformation of the hydrophilic (B) chains in ABA and BAB type triblock copolymers. Physica B: Condensed Matter, 2006, 385-386, 759-761.	2.7	1
382	Late-stage coarsening of oil droplets of excess oil in microemulsions following a temperature quench. International Journal of Materials Research, 2006, 97, 285-289.	0.8	1
383	Structure and dimerization of translation initiation factor aIF5B in solution. Biochemical and Biophysical Research Communications, 2011, 416, 140-145.	2.1	1
384	Effect of bisphosphonate treatment on subchondral bone nanostructure in the dunkin hartley guinea pig model of osteoarthritis studied by scanning small-angle X-ray scattering. Bone, 2012, 50, S117.	2.9	1
385	Polymorphism, Metastable Species and Interconversion. , 2014, , 373-386.		1
386	Formation of Dynamic Soluble Surfactant-Induced Amyloid Beta Peptide Aggregation Intermediates. Biophysical Journal, 2014, 106, 39a.	0.5	1
387	In Situ Smallâ€Angle Xâ€ray Scattering Investigation of the Formation of Dualâ€Mesoporous Materials. ChemPhysChem, 2015, 16, 3637-3641.	2.1	1
388	When Enzymes and Green Surfactants Meet. Biophysical Journal, 2016, 110, 211a.	0.5	1
389	Reply to Arlaud et al.: Structure of the C1 complex and the unbound C1r2s2 tetramer. Proceedings of the United States of America, 2017, 114, E5768-E5770.	7.1	1
390	Effect of concentration and ionic strength on the lower critical solution temperature of poly(N-isopropylacrylamide) investigated by small-angle X-ray scattering. Soft Materials, 0, , 1-9.	1.7	1
391	Scattering from Wormlike Micelles. , 2007, , 179-222.		1
392	Advancement of Fluorescent and Structural Properties of Bovine Serum Albumin-Gold Bioconjugates in Normal and Heavy Water with pH Conditioning and Ageing. Nanomaterials, 2022, 12, 390.	4.1	1
393	Surface relaxation by the keating model: A comparison with ab-initio calculations and x-ray diffraction experiments. Surface Science Letters, 1989, 210, A75-A76.	0.1	0
394	Small-angle neutron scattering of precipitates in Ni-rich Ni–Ti alloys. II. Methods for analyzing anisotropic scattering data. Erratum. Journal of Applied Crystallography, 1998, 31, 490-490.	4.5	0
395	XIth International Conference on Small-Angle Scattering. Journal of Applied Crystallography, 2000, 33, 0-0.	4.5	0
396	Impact Of Ceramide3 On POPC Host Membranes: A Study On Structure And Thermodynamics. Biophysical Journal, 2009, 96, 163a.	0.5	0

#	Article	IF	CITATIONS
397	Evidence of Coexisting Phases in Binary Mixtures of POPC/ceramide3. Biophysical Journal, 2010, 98, 667a.	0.5	0
398	Crystal growth in growing bone: Linking nanostructure with mineral density around the epiphyseal growth plate. Bone, 2012, 50, S116.	2.9	0
399	Liprotides: Nano-Sized Cytotoxic Protein-Fatty Acid Complexes with a Core-Shell or Multi-Layer Structure. Biophysical Journal, 2016, 110, 577a.	0.5	0
400	Liprotides: a New Class of Protein Lipid-Complexes. Biophysical Journal, 2016, 110, 577a.	0.5	0
401	Deducing the Relation between Viscosity and Oil-Induced Structural Changes of Viscoelastic Surfactants Using a Kinetic Approach. Journal of Physical Chemistry B, 2021, 125, 6306-6314.	2.6	0
402	Polymers at curved interfaces: microemulsions droplets decorated by block copolymers. Acta Crystallographica Section A: Foundations and Advances, 2002, 58, c11-c11.	0.3	0
403	Analysis of small-angle scattering data from block copolymer micelles using models based on Monte Carlo simulations. Acta Crystallographica Section A: Foundations and Advances, 2005, 61, c106-c106.	0.3	0
404	Small-angle scattering studies of freeze-dried silica gels. European Physical Journal Special Topics, 1993, 03, C8-353-C8-356.	0.2	0
405	Analysis of anisotropic SANS patterns obtained from Ni–Al–Mo alloys with bimodal particle size distributions. Acta Crystallographica Section A: Foundations and Advances, 1996, 52, C31-C31.	0.3	0
406	Structure of polymer-like micelles: SANS and Monte Carlo simulation studies. Acta Crystallographica Section A: Foundations and Advances, 1996, 52, C487-C487.	0.3	0
407	Late-stage coarsening of oil droplets of excess oil in microemulsions following a temperature quench. International Journal of Materials Research, 2022, 97, 285-289.	0.3	0